Methanofullerenes from Macrocyclic Malonates

Maurizio Carano,[a] Carlo Corvaja,[b] Luigi Garlaschelli,*[c] Michele Maggini,[d] Massimo Marcaccio,[a] Francesco Paolucci,*[a] Dario Pasini,[c] Pier Paolo Righetti,[c] Elena Sartori,[b] and Antonio Toffoletti[b]

Dedicated to Professor Paola Vita-Finzi on the occasion of her 70th birthday

Keywords: EPR spectroscopy / Fullerenes / Membranes / Sensors / Supramolecular chemistry

In this paper we describe the synthesis and intercomparison of several new methanofullerenes, each bearing a macrocyclic crown ether containing a malonate moiety directly attached to the C_{60}-fullerene core. Their complexing abilities with primary alkylammonium ions were investigated by NMR and mass spectrometry, and also by transport experiments through a liquid membrane. We also report on their electrochemical behaviour, together with EPR analysis of their supramolecular complexes with alkyl ammonium molecules labelled with a stable nitroxide radical.

Introduction

C_{60} derivatives have recently emerged in the scientific literature as promising new materials for various applications.[1] These have included the incorporation of C_{60} in molecular dyads[2] and triads,[3] as novel artificial photosynthetic systems, and − in combination with electroluminescent organic conjugated polymers − as components for all-organic solar cells.[4] Supramolecular systems incorporating C_{60} moieties have also been reported.[5]

Simple crown malonates such as 11,13-dioxo-13-crown-4 (**1a**) and its analogues **1b**−**d** were first prepared by Bradshaw et al.,[6] in order to study their cation complexing ability. Since then, these compounds have remained almost unexplored synthons in supramolecular chemistry, although the presence of the reactive methylene functionality offers easy potential access to a vast range of derivatives through all the typical reactions of malonic esters, whereas the crown ether structure can be appropriately modified to fit the complexation of different cations, with corresponding variation of the physicochemical properties of the complexes.[7]

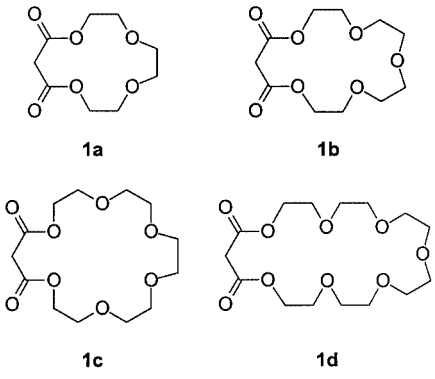

We have recently reported that crown ether derivatives incorporating a malonate unit and functionalised with π-electron-donating conjugated substituents to form ylidenemalonate moieties are able to form 1:1 complexes with Lewis acid-like metal cations, such as Mg^{2+} and Eu^{3+}, in organic solutions.[8] The complexation of the metal cation is essentially directed towards the conjugated 1,3-dicarbonyl system, but the ethylene glycol ether structure, depending

[a] Department of Chemistry "G. Ciamician", University of Bologna
Via Selmi, 2 40126 Bologna, Italy
E-mail: paolucci@ciam.unibo.it
[b] Department of Physical Chemistry, University of Padova
Via Loredan, 2 35131 Padova, Italy
E-mail: carlo.corvaja@unipd.it
[c] Department of Organic Chemistry, University of Pavia
Viale Taramelli, 10 27100 Pavia, Italy
Fax: (internat.) +39−0382 507323
E-mail: garlasch@chifis.unipv.it
[d] Department of Organic Chemistry, University of Padova
Via Marzolo, 1 35131 Padova, Italy
E-mail: michele.maggini@unipd.it

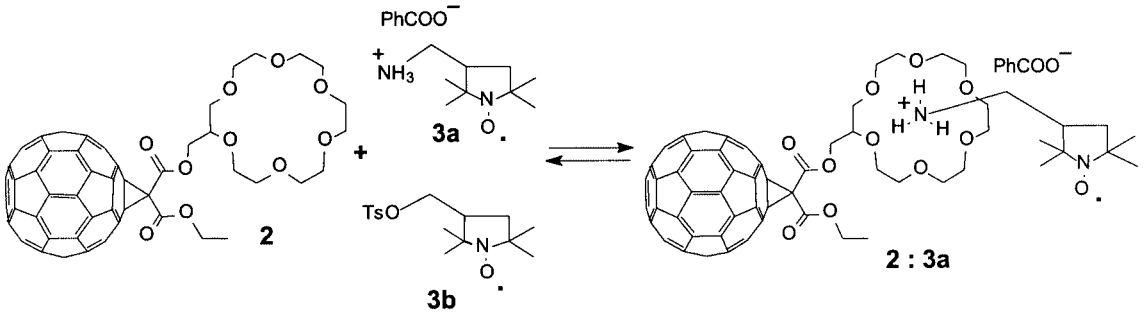

Figure 1. Non-covalent formation and EPR characterisation of radical triplet pairs formed by **2** and **3a**

on its chemical structure and overall dimensions, gives additional stabilisation to the 1:1 complex.

On the other hand, the Bingel reaction between the fullerene core and malonic esters has been widely used to obtain a number of methanofullerenes under mild conditions, in good yields and with high regioisomeric purities.[9] Furthermore, there are a number of known instances in which fullerenes have been connected to crown ethers to exploit the well-known complexing properties of these subunits.[10] It therefore also seemed interesting to prepare methanofullerenes from cyclic malonic esters and to explore their properties. In this context, we have also recently reported the synthesis of a malonate-derived methanofullerene bearing an 18-crown-6 moiety, as in **2**, and its photoinduced interaction with the PROXYL ammonium cation **3** as a guest (Figure 1), monitored by EPR spectroscopy.[5c,5d]

In this paper we report on the synthesis and intercomparison of several methanofullerenes each bearing a macrocyclic crown ether attached to the C_{60}-fullerene, their complexing abilities towards primary ammonium ions, their electrochemical behaviour, and their analysis by EPR techniques.

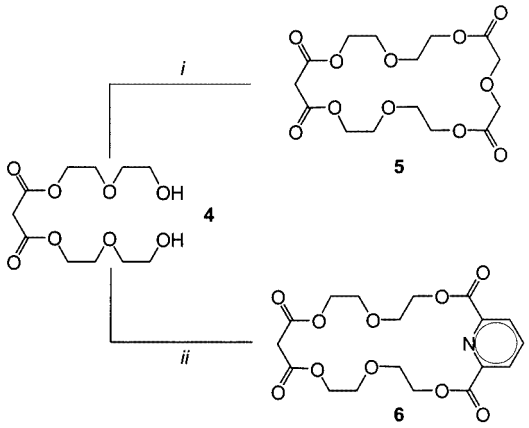

Scheme 1. Reagents and conditions: *i*) diglycolyl chloride, toluene, high dilution, Δ; *ii*) 2,6-pyridinedicarbonyl chloride, toluene, high dilution, Δ

Results and Discussion

Synthesis of the Components

The syntheses of crown ethers **1a**−**d** were carried out as described previously.[6b] We also modified the structure of crown ether **1d**, while preserving its overall structure at 22 atoms, through the insertion either of further "soft" carbonyl functionalities, as in the case of crown ether **5**,[8] or of a 2,6-pyridinedicarbonyl moiety, in order to ascertain possible cooperative effects in the stabilisation of suitable guests. The synthesis of the cyclic tetraesters **5** and **6**, each possessing a cyclic 22-atom structure, was performed according to Scheme 1.

Malonyl dichloride was treated with commercially available diethylene glycol monobenzyl ether. The malonic ester

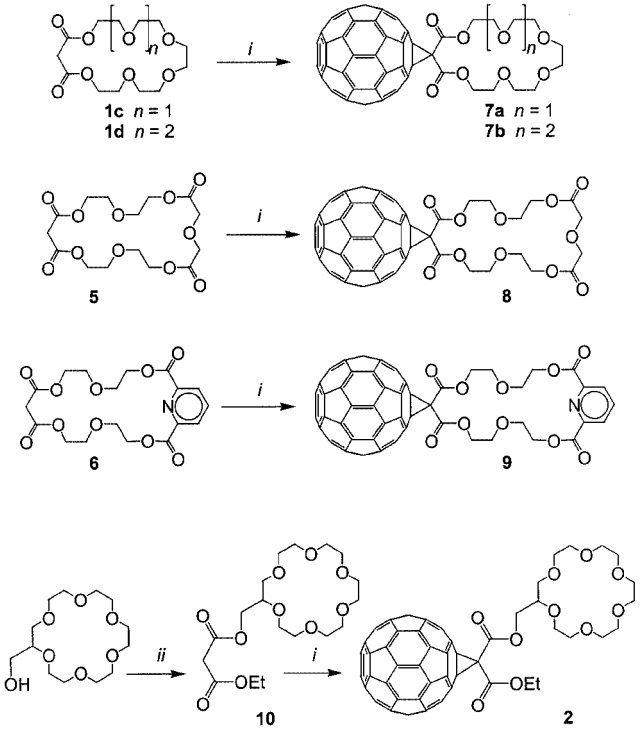

Scheme 2. Reagents and conditions: *i*) C_{60}, DBU, I_2, toluene, room temp.; *ii*) ethylmalonyl chloride, solid $NaHCO_3$, toluene, Δ

was then debenzylated by hydrogenolysis, and the resulting diol **4** was further treated, under high-dilution conditions, with the appropriate dicarboxylic acid dichloride. Methanofullerenes **7a**−**b**, **8** and **9** (Scheme 2) were obtained from malonates **1c**−**d**, **5** and **6**, respectively, and C_{60}-fullerene under standard Bingel conditions (room temperature, toluene, I_2, DBU) in 38 to 45% yields. They were purified by silica gel column chromatography and precipitated as dark amorphous solids on addition of MeOH. The malonate **10**, used for the synthesis of methanofullerene **2**, was obtained from commercially available hydroxymethyl-18-crown-6 and ethylmalonyl chloride as already described in a short report[5c] and as detailed in the Exp. Sect. All these fullerene derivatives showed good solubility in common organic solvents.

NMR, Complexation and Transport Studies

The complexing properties of **1c** in MeOH have been the subject of detailed investigations by Bradshaw and coworkers. Even though it showed a marked selectivity towards the binding of K^+ ions over Ba^{2+}, similarly to observations for the natural cyclic antibiotic valinomycin, the absolute thermodynamic binding constants were significantly lower than those recorded for, for example, 18-crown-6.

We have recently reported thermodynamic association constants, in MeCN solutions, between ylidenemalonate derivatives of crown ethers **1d** and **5** with selected metal cations, such as Mg^{2+} as its perchlorate salt and Eu^{3+} as its triflate salt. Since these compounds displayed strong intermolecular charge-transfer in the UV/Vis region, the association constants could be evaluated by UV/Vis titration procedures.

The UV/Vis spectra (in the 250−500 nm region) of fullerene derivatives **7b**, **8** and **9**, however, proved to be essentially superimposable on those obtained in 1 M MeCN solutions of Li^+, Mg^{2+}, Ba^{2+} and Sr^{2+} as their perchlorate salts. As would be expected, the lack of conjugation between the C_{60} core and the dicarbonyl system prevents any variation in the spectroscopic properties of the adducts, even though 1,3-dicarbonyl systems should be able to form at least weak complexes with the described Lewis acid-like cations such as Mg^{2+}.[11]

Crown ethers such as 18-crown-6 are well-known to give host/guest complexes with primary alkylammonium salts, in which the complex formation can be monitored by the chemical shift changes in both the crown and the alkylammonium protons.[12] In order to provide evidence of complexation for our components with ammonium salts, we therefore turned to ^{1}H NMR and mass spectrometry. When increasing amounts of benzylammonium perchlorate were added to solutions of **7a**−**b**, **8** and **9**, the only compound to show detectable variations in the NMR chemical shifts of some of the macrocyclic protons was **7b** (see Figure 2). For a 1:1 solution (10^{-3} M in $CDCl_3$) of **7b** and benzylammonium perchlorate (Figure 2, bottom), small but significant chemical shifts were recorded: ca. 0.1 ppm for the proton resonances in the α-position of the 1,3-diester unit, and ca. 0.05 ppm for the proton resonances associated with the β-protons.

Furthermore, the proton resonances associated with the γ-hydrogen atoms in the polyether chain (Figure 2) are split into four different groups of signals and undergo a maximum chemical shift variation of ca. 0.2 ppm. The formation of a complex between **7b** and the benzylammonium cation was also clearly substantiated by mass spectroscopic analysis of a 1:1 host/guest mixture in a $CHCl_3$ solution, showing the peak for the monocharged 1:1 adduct as the most abundant (1176 *m*/*z*, Figure 3). Attempts to evaluate

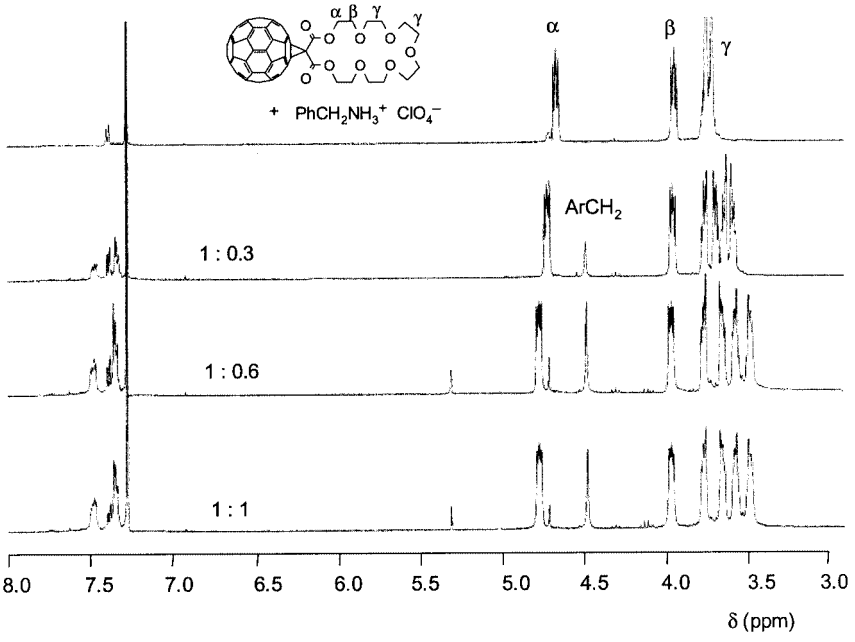

Figure 2. ^{1}H NMR spectra ($CDCl_3$, 300 MHz) of **7b** with increasing amounts of benzyl ammonium perchlorate

the association constants in $CDCl_3$ precisely were carried out by means of an NMR titration experiment, by addition of increasing amounts of the benzylammonium salt to a 10^{-3} M solution of fullerene crown ether **7b**. By fitting the data according to Equation (3) (see Exp. Sect.) we found a large standard deviation associated with the value of the binding constant (log $K_a = 2.7 \pm 1.0$ M^{-1}). The binding constant, however, seems to be dramatically lower than that reported for 18-crown-6 with a primary ammonium (methyl ammonium picrate) salt (log $K_a = 7.51$ M^{-1}), as determined by Cram's picrate extraction methodology.[13,14] Difficulties in measuring exact chemical shift differences of the peaks (which appear as multiplets, broadening with increasing addition of guest), together with the relatively small chemical shift variations upon complexation might be the cause of such large uncertainty in the nonlinear regression. Since all methanofullerene derivatives **7−9** absorb in the visible region, any attempt to quantify the binding constant with primary ammonium salts by picrate extraction (based on measures of picrate salt extracted in the organic phase, as determined by UV/Vis spectroscopic determination at 380 nm)[14] would have been inapplicable.

We therefore turned our attention to liquid membrane transport experiments, which have been used as a valuable tool for the evaluation of recognition phenomena in supramolecular chemistry.[15] The receptor, which is soluble in the underlying organic phase, is used as a carrier for the transport of metal or ammonium ions (usually as picrate salts) between one aqueous phase (the source phase) to another aqueous phase (the receiving phase).[15b] Since the picrate salt of benzyl ammonium ion showed poor solubility in H_2O ($< 10^{-3}$ M), we chose to use the simplest primary ammonium ion, methyl ammonium picrate, which has a good solubility in H_2O ($> 10^{-2}$ M), and has been used by numerous other research groups. The results, summarised in Table 1, refer to the relative initial linear transport rate through the U-tube apparatus.[16] As is evident, the methanofullerenes derived from malonate crown ethers all have substantially lower rates of transport for methylammonium picrate than the 18-crown-6 fullerene derivative **2**.

Table 1. Comparison of methylammonium picrate transport across a $CHCl_3$ bulk liquid membrane at 20 °C in the presence of C_{60} hosts.

Entry[a]	Carrier	Transport rate (μmol/h)	Relative transport rate
1	–	0.0088[b]	1
2	18-crown-6	4.786	544
3	2	1.118	127
4	7a	0.0136	1.55
5	7b	0.0408	4.63
6	8	0.0130	1.48
7	**9**	0.0273	3.10

[a] The values reported are the result of initial transport rates with linear regressions giving high-confidence outputs ($r^2 > 0.99$). See Exp. Sect. for details. [b] A replicate experiment gave a result of 0.091.

The value in entry 2, for crown ether 18-crown-6, is much higher value than that for compound **2** (entry 3), also as a result of better partition in the aqueous phase, which should facilitate dissolution of the picrate in the organic phase and consequent transport.

Since partition of all these fullerene derivatives between the organic and aqueous phases under the experimental conditions used is negligible, as they remain completely in the organic phase,[17] the values in entry 3−7 could be regarded as a qualitative measure of the corresponding receptor ability to bind the primary ammonium salt in the organic phase, and therefore to transport it into the receiving aqueous phase. A blank experiment, conducted without any carrier present in the organic phase, showed a detectable transport rate (entry 1 in Table 1), as a result of the residual solubility of the picrate methylammonium salt in the organic phase, well documented in the literature.[14]

Transport rates for fullerene derivatives **7b−9**, possessing the same overall crown ether dimensions of 22 atoms, do

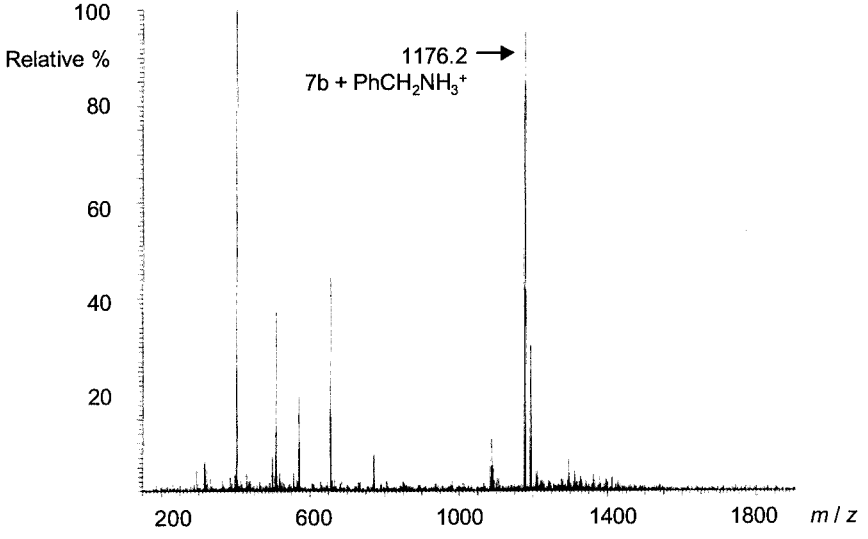

Figure 3. Mass spectroscopic characterisation (ESI) of an equimolar mixture of **7b** and benzylammonium perchlorate

show marked relative differences, compound **7b** being the most efficient.

The fact that **7b** shows transport rates superior to those of **7a** suggests that the presence of a sufficient number of purely ethereal oxygen atoms is a necessary requisite for complexation through H bonds to occur − according to the accepted model − on alternate oxygens.[6c]

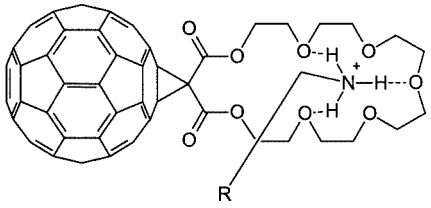

On the other hand, small changes within the crown ether structure (the introduction, for example, of two additional carbonyl functionalities as in compounds **8** or **9**, possessing the same overall crown ether dimensions of 22 atoms as **7b**) seem to bring about a drastic reduction in the complexing ability towards primary ammonium ions, possibly owing to an increased rigidity of the ring.

EPR Studies

In order to test the formation of host/guest complexes of alkyl ammonium ions and fullerene crown ethers in solution, a new method was devised, exploiting the high-yield generation of long-lived triplet excitation localised on C_{60}. The method consists of the use of alkylammonium molecules labelled with a stable nitroxide radical, the unpaired electron of which would be able to interact with the triplet excited fullerene spin. The coupling of the triplet spin (S = 1) with the free radical spin (S = 1/2) generates two states with total spins S = 3/2 (quadruplet) and S = 1/2 (doublet). In principle, both states can be observed and be distinguished in solution by TR-EPR. In fact, they have characteristic g factors and hyperfine splitting constants, quite different from those of the separated triplet and radical species.[18] The doublet is not usually detected, however, due to its short lifetime.

In order to understand the relevant features of nitroxides' and C_{60} derivatives' TR-EPR spectra, reported in Figures 4−6, we present a brief description of the interaction processes taking place between a stable free radical and a photoexcited triplet state. The graphics refer to the systems consisting of the triplet excited derivatives **2**, **7a** and **7b** in the presence of the nitroxide radical **3b** and of radical **3a**, which bears an alkylammonium group. It has been already shown that the latter is able to complex with the crown ether moiety of **2**.[5c] These systems were chosen because they display all relevant aspects of the processes described below more clearly.[19]

Upon absorption of visible light, the C_{60} moiety is excited into a singlet state, and is transformed into the first excited triplet state T by a fast ($k_{ISC} = 8 \times 10^{10}$ s^{-1}) and very efficient intersystem crossing (ISC) process ($\Phi_{ISC} > 0.9$).

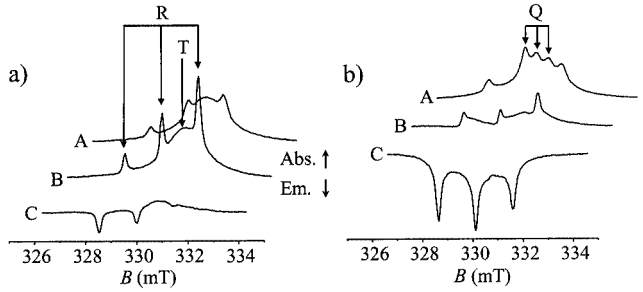

Figure 4. a) TR-EPR spectra of a 1:1 2 mM $CHCl_3$ solution of **2** and **3b**; R indicates the three hyperfine lines of the nitroxide free radical; T indicates the line of the fullerene excited triplet state; sections extracted from a 2D (time and magnetic field)-TR-EPR surface at different delays from the laser pulse: A) 0.3 μs, B) 0.5 μs, C) 3.5 μs; b) TR-EPR spectra of a 1:1 2 mM $CHCl_3$ solution of **2** and **3a**; Q indicates the three lines of the excited quadruplet state; sections extracted from a 2D (time and magnetic field)-TR-EPR surface at different delays from the laser pulse: A) 0.3 μs, B) 0.5 μs, C) 3.0 μs

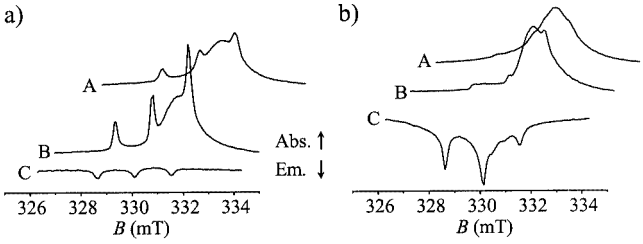

Figure 5. a) TR-EPR spectra of a 2 mM 1:1 $CHCl_3$ solution of **7b** and **3b**; sections extracted from a 2D (time and magnetic field)-TR-EPR surface at different delays from the laser pulse: A) 0.3 μs, B) 0.5 μs, C) 3.5 μs; b) TR-EPR spectra of a 1:1 2 mM $CHCl_3$ solution of **7b** and **3a**; sections extracted from a 2D (time and magnetic field)-TR-EPR surface at different delays from the laser pulse: A) 0.3 μs, B) 0.5 μs, C) 2.0 μs

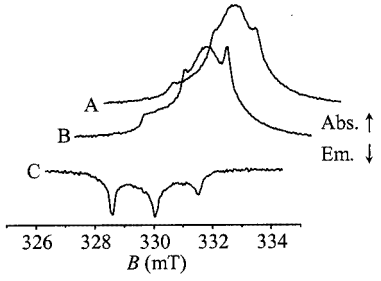

Figure 6. TR-EPR spectra of a 2 mM 1:1 $CHCl_3$ solution of **7a** and **3b**; sections extracted from a 2D (time and magnetic field)-TR-EPR surface at different delays from the laser pulse: A) 0.3 μs, B) 0.5 μs, C) 3.5 μs

The triplet state at zero magnetic field (B = 0) is split in the sub-states, $|X\rangle$, $|Y\rangle$ and $|Z\rangle$, the energies of which are the eigenvalues of the electron dipolar interaction. ISC is anisotropic: the populating rates of the individual triplet sublevels are different. The populations of the zero field states generated by a laser light pulse thus deviate from the thermal equilibrium values. In fullerene monoadduct derivatives, the populating rates are typically in the ratios

P_x:P_y:P_z = 0.1:1:0.01, with the triplet $|Z>$ being less populated than the others.

In the high magnetic field of an EPR spectrometer ($B \neq 0$), the zero field states $|X>$ $|Y>$ and $|Z>$ are transformed into the T_{-1}, T_0 and T_1 states, characterised by the projection of the spin angular momentum along the magnetic field direction. The transformation depends on the orientation of B with respect to the molecular axis system.

For an oriented system, the populating rates of the T_i ($i = -1,0,1$) is expressed by Equation (1):

$$k_i = \Sigma k_j |< T_i | j >|^2 \, (j = x,y,z) \quad (1)$$

In liquid solution of low viscosity, the fast molecular rotational diffusion ($\tau_C \approx 10^{-11}$ s) scrambles the initial populations of the states T_{-1}, T_0 and T_1, corresponding to a random distribution of molecular orientations. Moreover, the transitions $T_{-1} \Leftrightarrow T_0$ and the $T_0 \Leftrightarrow T_1$ EPR become degenerate and the system behaves as a two-level (α and β) system, the spin polarisation P of which is expressed by Equation (2).[20]

$$P = (n_\alpha\text{-}n_\beta)/(n_\alpha + n_\beta) = (4/15)\,(D/B)\,(P_x + P_y - 2P_z) \quad (2)$$

For C_{60} monoadducts ($D \cdot -9.5$ mT), P is negative and the liquid solution EPR signal of their triplet state results in enhanced absorption, as is clearly visible (broad line at $g_T = 2.001$, indicated as T) in Figure 4, part a (curves A and B), referring to derivative **2**.

The triplet spin polarisation can be transferred to free radicals present in solution. Electron spin polarisation transfer (ESPT)[5d,21] is a very fast process, taking place in the first instants after the triplet generation and responsible for the absorptive character of the three hyperfine nitroxide lines (g_{NO}·· 2.006, a_N·· 1.5 mT), clearly visible (R) in Figure 4, part a (curves A and B), referring to nitroxide **3b** in the presence of derivative **2**.

A second effect of radical triplet interaction derives from the formation of radical triplet pairs [RTP], which may be formed either in a quadruplet or in a doublet state. RTPs in the doublet state decay very rapidly to the ground state fullerene and radical, while this process is spin-prohibited for RTPs in the quadruplet state. It becomes partially allowed by the state mixing caused by the electron spin dipolar interaction.[22]

Since the mixing is selective for the electron spin component along the magnetic field, the $S_z = \pm 1/2$ radical substates become populated at different rates.

The radical triplet pair mechanism (RTPM) theory predicts an excess of population in the high-energy $S_z = 1/2$ state, if the radical triplet exchange interaction J is negative, as is usually the case.[22b,22c,23]

The polarisation inversion of the lines (passing from τ = 0.5 μs, curve B, to τ = 3.5 μs, curve C) shown in Figure 4 (part a) is due to this second process, which produces emissive polarisation. In the case of **3b** and excited triplet **2**, the RTP is a collision complex that dissociates very rapidly and cannot be observed, while with **3a**, three additional EPR lines appear in the spectrum recorded at 235 K (indicated with Q in curve A of Figure 4, b). They are attributable to the RTP in the metastable quadruplet state. In fact, they have $g = (g_{NO} + 2g_T)/3$, as predicted by theory.[24] With increasing temperature the spectrum becomes less resolved.

For derivatives **7a** and **7b**, the behaviour with **3b** is the same: the excited triplet signal is recorded together with nitroxide lines, which reverse their phase later (Figure 5, part a, only **7b** is shown). With **3a**, derivative **7b** also shows the three lines of the quadruplet RTP (Figure 5, part b), albeit less resolved than for **2**. A better resolution can be achieved by performing the first derivative of the signal intensity with respect to the magnetic field intensity (not shown in the Figure). Derivative **7a** shows the nitroxide lines superimposed to a broad feature, but the quadruplet lines are not resolved (Figure 6).

The linewidth is in any case much larger than that measured for RTP in rigid systems in which radical and triplet were bound by rigid covalent bonds.[18] A possible explanation is the occurrence of association/dissociation equilibrium of the RTP. Further investigation on the lineshape is in progress. The experiments show that C_{60} crown malonates form host/guest complexes with ammonium nitroxide, although − presumably − to a minor extent with respect to C_{60} crown ether. The influence of macrocycle dimension and structure on the process is therefore confirmed.

Electrochemical Studies

The electrochemical properties of methanofullerenes **7a**−**b**, **8** and **9** were investigated up to highly negative potentials in THF at low temperature and under strictly aprotic conditions.[25]

Figure 7, part a shows the cyclic voltammetric (CV) curve of a 0.5 mM solution of **8** in THF at −55 °C and v = 0.5 V/s. The CV curve displays six reduction peaks, denoted by Roman numbers, showing either reversible or irreversible features. In particular, peaks II, III and IV are irreversible, since their i_{pa}/i_{pc} ratios are greatly lower than one, and, additionally, two extra anodic peaks are observed in the reverse scan (at −1.09 and −1.70 V) but lack a cathodic counterpart in the forward scan: such features would attest to the occurrence of a chemical reaction coupled to some of the reduction processes, in line with the known reactivity of multiply reduced bis(alkoxycarbonyl)methanofullerene derivatives (vide infra).[26] An almost identical CV pattern was observed for **7a** and **7b**, thus suggesting that all the redox processes are located on the methanofullerene moiety and that the structure of the addend has no significant effect on its redox properties. Conversely, the CV curve of **9** (Figure 7, part b) displays, superimposed to a CV pattern as in the previous species, an additional cathodic peak (denoted by an asterisk) at −1.90 V and a corresponding anodic one at −1.82 V, thus comprising a reversible redox couple with $E_{1/2}$ = −1.86 V. On comparison with the CV curve of **6**, obtained under the same conditions as for Figure 7, part b, which shows a single reduction peak at −1.91

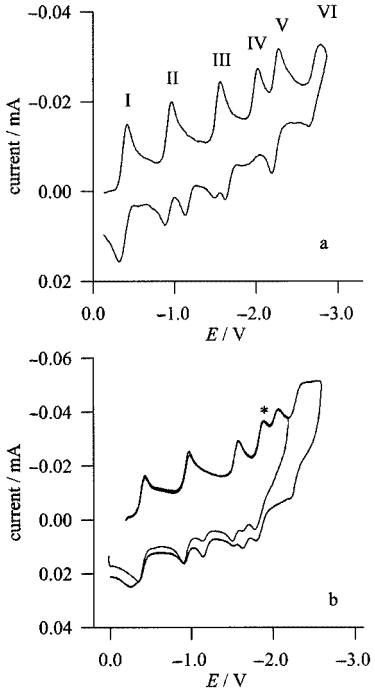

Figure 7. CV curve of a 0.5 mM **8** (a), or **9** (b), 0.05 M TBAH THF solution; scan rate: 0.5 Vs^{-1}; $T = -55$ °C; working electrode: platinum disk microelectrode (125 μm diameter)

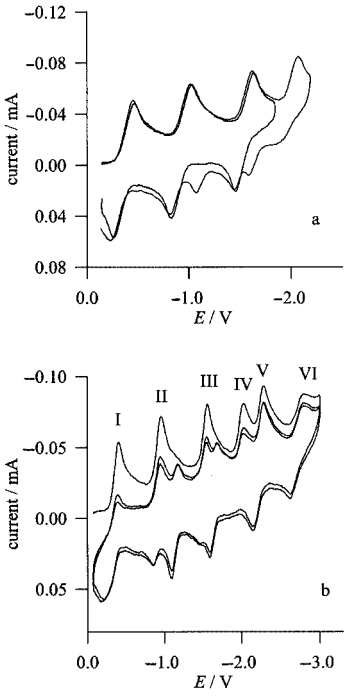

Figure 8. CV curve of a 0.5 mM **8**, 0.05 M TBAH THF solution; scan rate: 5 Vs^{-1}; $T = -55$ °C; working electrode: platinum disk microelectrode (125 μm diameter)

V, the additional reduction process in **9** was attributed to the pyridine moiety.

As anticipated above, the presence of irreversible cathodic peaks in the forward scans and of extra anodic peaks in the reverse scans in the CV curves of the above species confirmed the occurrence of a follow-up chemical reaction coupled to the fullerene-centred reductions. Further details relative to the electrode mechanism responsible for such a CV pattern were obtained by performing CV experiments as a function of scan rate, temperature and reversal potential.

Figure 8 (parts a and b) display the CV curves of **8**, obtained under the conditions of Figure 7 but at higher scan rate (5 V/s) and including a varying number of reduction peaks. The curves show that:

(i) The extra anodic peaks at −1.09 and −1.70 V are due to some species that is generated from the pristine species following the fourth (irreversible) reduction of the fullerene moiety (Figure 8, a), and, accordingly, peaks V and VI in Figure 8, part b should also be attributed to such a novel species,

(ii) The cathodic counterparts of the anodic peaks at −1.09 and −1.70 V are observed when a second cathodic scan is carried out without the renewal of the diffusion layer (Figure 8, b), thus allowing the determination of the corresponding $E_{1/2}$ values (−1.13 and −1.64 V, respectively),

(iii) As the scan rate is increased (compare Figure 7, part a and Figure 8, part b), the height of the extra anodic peaks increases at the expense of the anodic counterparts of peaks II and III, due to the pristine species; such a scan rate dependence of the CV pattern, together with the fact that in the subsequent scans (Figure 8, b) the curve consistently remains the same as in the second scan, would suggest that under these conditions the follow-up chemical reaction described in (i) is partly reversed upon performing the oxidation scan.

It is known that bis(alkoxycarbonyl)methanofullerene derivatives (Bingel adducts) undergo the removal of the cyclopropane ring under bulk electrolysis conditions, yielding the pristine fullerene (retro-Bingel process).[26] The hypothesis that the novel species responsible for the redox processes at −1.09 and −1.70 V, as well as for peaks V and VI in the CV curves of Figure 8, may be identified with C_{60} was dismissed, however, because under the same conditions the latter undergoes six subsequent reductions: at −0.38, −0.95, −2.53, −2.02, −2.55 and −3.01 V.[25a] In view of the relatively slow kinetics of the retro-Bingel process,[26d] the above species should rather be identified with the corresponding fullerene derivatives in which one of the cyclopropane bonds has been cleaved, a step that would be reversible on the CV timescale and is thought to be preliminary to the retro-Bingel reaction.[26,27]

Such a hypothesis was verified by performing CV experiments at high temperature. The CV curves of **8** obtained under the conditions of Figure 8 but at 25 °C are shown in Figure 9. Comparison of the CV curves in Figures 8 and 9 suggests that the reactivity observed at the level of the tetraanion at low temperature is anticipated, at high temperature, at the level of the third reduction.

Figure 9 (part a) in fact shows that, while the first two reduction peaks of **8** are reversible, the third peak is irre-

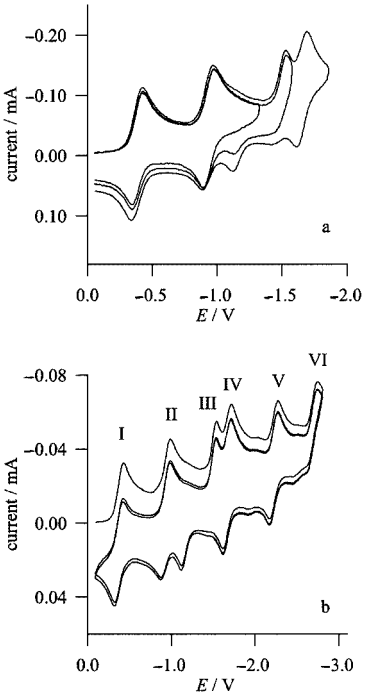

Figure 9. CV curve of a 0.5 mM **8**, 0.05 M TBAH THF solution; scan rate: 5 Vs^{-1}; T = 25 °C; working electrode: platinum disk microelectrode (125 μm diameter)

versible and gives rise to the anodic peak at −1.09 V, also observed in the CV curves at low temperatures following the fourth reduction process (Figure 8, a). In addition, peaks V and VI coincide with those observed at low temperature, substantiating the hypothesis that such peaks have to be attributed to the novel species forming from the multiply reduced methanofullerene. At variance with the behaviour at low temperature, the second and successive scans performed without renewal of the diffusion layer display CV patterns that coincide with that obtained in the first scan (Figure 9, b). Importantly, under the conditions of Figure 9 (b), the cathodic counterpart of the anodic peak at −1.09 V is not observed, at odds with the behaviour at −55 °C (Figure 8, b). This confirms the above hypothesis that the follow-up reaction coupled to the multiple reduction, either the third (at, 25 °C) or the fourth one (at −55 °C), of the above species is reversed upon reoxidation.

Further work aimed at isolating and identifying the transient species involved in the redox processes is in progress. The elucidation of the electrode mechanism evidenced by the CV experiments is beyond the scope of this paper, however, and will be the subject of forthcoming publications.[28]

Conclusions

This study illustrates the synthesis and characterisation of fullerene derivatives bearing macrocyclic malonates directly attached to the C_{60} core through a cyclopropane moiety. NMR and mass spectrometry have confirmed that some of these compounds are able to form 1:1 complexes with primary ammonium ions. The transport properties of these compounds have shown that small structural variations within the crown ether structure have a profound effect on their ability to bind primary ammonium ions.

We have confirmed by TR-EPR that **7b** gives ammonium complexes as shown by the NMR investigation described in the previous section. TR-EPR indicates that some association should also take place for **7a**.

In this regard, the CV investigation carried out on species **7a**, **7b**, **8** and **9** has shown that the injection of three (at 25 °C) or four (at −60 °C) electrons triggers a follow-up reaction responsible for irreversible CV behaviour; such a reaction is, however, reversed upon re-oxidation with relatively low scan rates. This implies that the transient chemical species generated by the reduction of the above species, and presumably to be identified with the corresponding fullerene derivatives in which one of the cyclopropane bonds has been cleaved, a step believed to be preliminary to the so-called retro-Bingel reaction,[26,29] are stable on the relatively long timescales of CV.

Experimental Section

General Remarks: Compounds **3a**,[5d] **3b**,[5c] **5**[8] and **7b**[30] were synthesised as described previously. All commercially available compounds were purchased from Aldrich and used as received. Benzene (Na), THF (CaH_2) and CH_2Cl_2 (CaH_2) were dried and distilled before use. Tetrabutylammonium hexafluorophosphate (TBAH, puriss. from Fluka) was used as supporting electrolyte as received. Tetrahydrofuran (THF, LiChrosolv, Merck) used for the electrochemical experiments was treated according to a procedure described elsewhere:[18] the solvent was distilled into the electrochemical cell prior to use, by a trap-to-trap procedure. ^1H and ^{13}C NMR spectra were recorded from solutions in $CDCl_3$ or CD_3CN on Bruker 200 or AMX 300 machines with the solvent residual proton signal or tetramethylsilane (TMS) as a standard. Infrared spectra were recorded on a Perkin−Elmer 881 in NaCl disks. Mass spectra were recorded in an Electrospray Ionization LCQ Deca (Thermofinnigan) instrument. The UV/Vis spectroscopic studies were conducted on a Perkin−Elmer Lambda 5 spectrophotometer. Melting points were recorded on a Büchi 510 apparatus and are uncorrected.

Association Constant Experiments and Transport Studies: MeCN (Carlo Erba UV/Vis spectroscopic grade) was used for UV/Vis spectrophotometric studies. A Mettler H31 analytical balance (with a precision of 10^{-4} g) was used to weigh the samples for the stock solutions. Aliquots of these stock solutions were then taken by high-precision Hamilton syringes to prepare the samples for NMR and UV/Vis spectroscopic analyses.

Titration Experiments. The titration experiments were conducted as follows: to a stock solution of fullerene-crown ether (solution A) in $CDCl_3$ were added several aliquots of a solution (solution B) of the benzylammonium perchlorate salt (at higher concentration) dissolved in solution A, in order to maintain the crown ether always at the same, constant concentration. Stock solutions A were 1×10^{-3} M, whereas stock solution B were 1.4×10^{-3} M in $CDCl_3$. After each addition, the ^1H NMR spectrum (300 MHz) in $CDCl_3$ was recorded and the chemical shift variations (Δδ, in Hz) upon the addition of the benzylammonium salts were measured. By em-

ployment of a nonlinear fitting curve program, the plot of $\Delta\delta$ against the metal concentration x was fitted by Equation (3),[8,14b] to afford the value of the association constant k_a.

$$\Delta\delta = (\Delta\delta_{max}/C)\ \frac{k_a(C+x)+1-[[k_a(C+x)+1]2-4k_a{}^2 C\,x]^{0.5}}{2k_a} \quad (3)$$

$\Delta\delta$ is the measured chemical shift difference, x is the total concentration of methylammonium salt added, $\Delta\delta_{max}$ is the chemical shift difference in conditions of complete complex formation, C is the total concentration of the titrate (the crown ether), and k_a is the association constant for the 1:1 complex.

Transport Experiments: Methylammonium picrate was synthesised from methylamine and picric acid and purified by recrystallisation from MeOH (m.p. 211 °C, ref.[31]: 211 °C). The source phase comprised a 10 mM aqueous solution of methylammonium picrate (7 mL), while the receiving phase was distilled water (7 mL). The liquid membrane was a 1 mM solution of the appropriate crown ether host (15 mL). The same membrane vessel and the same stirring rate (100 rpm) were used throughout this study. Aliquots were taken from the receiving phase (100 μL) at periodic intervals and dissolved in MeCN (1.5 mL), and the absorbance at 380 nm was recorded. By use of the molar absorptivity of methylammonium picrate in MeCN (ε_{380} = 26000 dm^3 mol^{-1} cm^{-1}, ref.[14] = 17400), the quantity of guest transported could be calculated and the transport rate (in μmol/h) evaluated through a simple least-square linear regression.

EPR Measurements: Solutions of about $2\cdot10^{-3}$ M concentration in $CHCl_3$ (Prolabo) were prepared directly in the quartz EPR tubes (outer diameter: 3 mm) and carefully deoxygenated by several freeze/pump/thaw cycles. EPR spectra were recorded on a CW-EPR spectrometer (Bruker ER 200 D) operating in the X band and equipped with a liquid nitrogen cryostat. Time-resolved EPR measurements were performed by collecting the signal with a digital oscilloscope (LeCroy 9450A or LeCroy Waverunner LT344) without using the 100 kHz field modulation. Photoexcitation was achieved by irradiation of the samples, inside the cavity of the spectrometer, with 20 ns light pulses from an excimer XeCl laser (Lambda Physik LPX 100, λ = 308 nm) pumping a dye (Rhodamine 6G) laser (Lambda Physik FL 2000, λ = 582 nm) or with 5−6 ns light pulses from a Nd:YAG Q-switched laser (Quantel Brilliant, λ = 532 nm). Field-time two-dimensional surfaces were obtained in the following way: one transient EPR signal was recorded at a fixed field position, averaged (100−200 times), and stored in a PC. The field was then incremented and the process was repeated for different field positions. In-house software was used to control the field steps and data acquisition.

Electrochemical Instrumentation and Measurements: The CV experiments were carried out according to procedures described elsewhere.[18] Potentials were measured with respect to the ferrocene standard and are always referred to saturated calomel electrode (SCE). $E_{1/2}$ values correspond to $(E_{pc}+E_{pa})/2$ from CV. For irreversible peaks, the peak potential, E_p, is given, measured at 0.5 V s^{-1}. Ferrocene was also used as an internal standard for checking the electrochemical reversibility of a redox couple. Voltammograms were recorded with a AMEL Model 552 potentiostat or a custom-made fast potentiostat controlled either by an AMEL Model 568 function generator or by an ELCHEMA Model FG-206F. Data acquisition was performed with a Nicolet Model 3091 digital oscilloscope interfaced to a PC. Temperature control was accomplished within 0.1 °C with a Lauda thermostat.

Compound 2:[5c] Compound **10** (90 mg, 0.22 mmol), C_{60} (180 mg, 0.25 mmol) and I_2 (61 mg, 0.24 mmol) were dissolved in toluene (140 mL). A solution of DBU (1,8-diazabicyclo[5.4.0]undec-7-ene, 84 mg, 0.55 mmol) in toluene (5 mL) was added dropwise at room temperature over a period of 15 min. After stirring overnight, the reaction mixture was purified by column chromatography (SiO_2; toluene, then toluene/MeOH, 95:5) to obtain **2** as a dark brown solid (50 mg, 20%). M.p. > 250 °C. ^{1}H NMR (400 MHz, $CDCl_3$): δ = 1.49 (t, 3 H, −COOCH$_2$C*H*$_3$), 4.07−3.60 (m, 23 H, −OC*H*$_2$CH$_2$O−), 4.57 (q, 2 H, −OOC*H*$_2$CH$_3$), 4.67 (d, 2 H, −COOC*H*$_2$CH−) ppm. ^{13}C NMR ($CDCl_3$): δ = 14.0, 14.3, 22.6, 63.6, 65.8, 66.6, 68.1, 69.2, 69.9, 70.0, 70.1, 70.4, 70.6, 138.9, 139.0, 139.0, 140.9, 140.9, 141.7, 141.8, 141.8, 142.1, 142.1, 142.9, 143.0, 143.0, 143.0, 143.8, 144.6, 144.6, 144.6, 144.6, 144.8, 145.0, 145.0, 145.1, 145.1, 145.1, 145.2, 163.5, 163.5 ppm. UV/Vis (CH_2Cl_2): λ_{max} (ε/dm^3 mol^{-1} cm^{-1}) = 324 (2700), 257 (8570), 226 (71400) nm. MS (ESI): *m*/*z* = 1149 [M + Na]$^+$, 1165 [M + K]$^+$.

Compound 6: Diol **4**[8] (5.7 g, 20.3 mmol), dissolved in benzene/THF (1:1, 80 mL), and pyridine-2,6-dicarbonyl chloride (4.15 g, 20.3 mmol), dissolved in benzene/THF (1:1, 80 mL), were slowly added from identical dropping funnels over a 10 h period to a toluene (400 mL) solution kept at 55 °C. The reaction vessel was equipped with a NaOH trap. After the mixture had cooled, the solvent from the reaction mixture was reduced by half, and the solution was washed twice with a saturated $NaHCO_3$ solution. The aqueous phase was extracted with CH_2Cl_2, and the crude reaction mixture was purified by column chromatography (SiO_2; EtOAc). The reaction mixture was stirred vigorously for 4 days, and then cooled to room temperature. The solvent was distilled off at reduced pressure, and the oily residue was then subjected to purification. Yield: 3.66 g (44%). M.p. 127−129 °C (EtOAc). IR: $\tilde{\nu}$ = 1736 (ν_c = $_o$),1719 (ν_c = $_o$) cm^{-1}. ^{1}H NMR ($CDCl_3$): δ = 8.32 (d, 2 H, Py*H*), 8.02 (t, 1 H, Py*H*), 4.63−4.53 (m, 4 H, −COOC*H*$_2$CH$_2$O−), 4.36−4.26 (m, 4 H, −COOC*H*$_2$CH$_2$O−), 3.87−3.96 (m, 4 H, −COOCH$_2$C*H*$_2$O−), 3.78−3.86 (m, 4 H, −COOCH$_2$C*H*$_2$O−), 3.38 (s, 2 H, −OOCC*H*$_2$COO−) ppm. ^{13}C NMR ($CDCl_3$): δ = 166.9, 165.0, 148.6, 138.6, 128.5, 69.4, 69.3, 65.5, 65.1 ppm. $C_{18}H_{21}NO_{10}$: calcd. C 52.6, H 5.2, N 3.4; found C 52.2, H 5.6, N 3.1.

Compound 7a: DBU (76 mg, 0.5 mmol) in toluene (5 mL) was added to a solution of **1c** (60 mg, 0.2 mmol), C_{60} (145 mg, 0.2 mmol) and I_2 (50 mg, 0.2 mmol) in toluene (130 mL), and the mixture was stirred for 12 h under nitrogen. The reaction mixture was purified by column chromatography (SiO_2; toluene, to remove unchanged C_{60}, then toluene/*i*PrOH, 9:1) to obtain **7a** as a dark brown solid (92 mg, 45%). M.p. > 250 °C. IR: $\tilde{\nu}$= 2923, 1742, 1428, 1232, 1119 cm^{-1}. ^{1}H NMR (400 MHz, $CDCl_3$/CD_3CN, 7:3): δ = 4.48 (m, 4 H, −COOC*H*$_2$CH$_2$O−), 3.77 (m, 4 H, −COOCH$_2$C*H*$_2$O−), 3.56 (m, 12 H, −OC*H*$_2$CH$_2$O) ppm. ^{13}C NMR ($CDCl_3$): δ = 163.4, 145.2, 145.1, 145.0, 144.8, 144.6, 144.5, 144.5, 143.8, 143.0, 142.9, 142.9, 142.1, 141.8, 140.8, 139.0, 71.4, 71.0, 70.9, 70.8, 68.6, 66.4, 51.7, 30.8 ppm. UV/Vis ($CHCl_3$): λ_{max} (ε/dm^3 mol^{-1} cm^{-1}) = 426 (6000), 326 (40600), 258 (135740) nm. MS (ESI): *m*/*z* = 1042.4 [M + NH$_4$]$^+$, 1047.5 [M + Na]$^+$, 1063.3 [M + K]$^+$.

Compound 8: Compound **5** (70 mg, 0.185 mmol), C_{60} (145 mg, 0.2 mmol), and I_2 (61 mg, 0.24 mmol) were dissolved in toluene (120 mL). A solution of DBU (76 mg, 0.5 mmol) in toluene (5 mL) was added dropwise at room temperature over a period of 15 min.

After stirring overnight, the reaction mixture was purified by column chromatography (SiO_2; toluene, then toluene/*i*PrOH, 95:5) to obtain **8** as a dark brown solid (91 mg, 45%). M.p. > 250 °C. IR: $\tilde{\nu}$ = 2920, 1740, 1440, 1230, 1140 cm $^{-1}$. ^{1}H NMR (400 MHz, $CDCl_3$): δ = 4.46 (m, 4 H, −COOCH_2−), 4.17 (m, 4 H, −COOCH_2−), 4.14 (s, 4 H, −COOCH_2OCH$_2$OOC−), 3.60 (m, 4 H, −COOCH$_2$CH_2−), 3.70 (m, 4 H, −COOCH$_2$CH_2−), 3.60 (m, 4 H, −COOCH$_2$CH_2−) ppm. ^{13}C NMR ($CDCl_3$): δ = 169.7, 163.4, 145.2, 145.1, 145.0, 144.6, 143.8, 143.0, 142.1, 141.8, 140.9, 139.0, 68.8, 68.5, 68.1, 65.8, 63.8 ppm. UV/Vis ($CHCl_3$): λ_{max} (ε/dm^3 mol^{-1} cm^{-1}) = 462 (5270), 427 (5630), 326 (40000), 257 (141600) nm. MS (ESI): *m*/*z* = 1114.1 [M + NH$_4$]$^+$, 1119.3 [M + Na]$^+$.

Compound 9: Compound **6** (82 mg, 0.2 mmol), C_{60} (145 mg, 0.2 mmol), and I_2 (61 mg, 0.24 mmol) were dissolved in toluene (120 mL). A solution of DBU (76 mg, 0.5 mmol) in toluene (5 mL) was added dropwise at room temperature over a period of 15 min. After stirring overnight, the reaction mixture was purified by column chromatography (SiO_2; toluene, then toluene/*i*PrOH, 95:5) to obtain **9** as a dark brown solid (86 mg, 38%). M.p. > 250 °C. IR: $\tilde{\nu}$ = 2950, 1745, 1725, 1437, 1320, 1243, 1138 cm $^{-1}$. ^{1}H NMR (400 MHz, $CDCl_3$): δ = 3.76 (m, 4 H, COOCH$_2$CH$_2$), 3.84 (m, 4 H, COOCH$_2$CH$_2$), 4.39 (m, 4 H, COOCH$_2$), 4.54 (m, 4 H, COOCH$_2$), 7.86 (t, 1 H, Ar), 8.12 (d, 2 H, Ar) ppm. ^{13}C NMR ($CDCl_3$): δ = 164.8, 148.0, 145.1, 144.6, 143.8, 142.9, 142.1, 141.8, 140.8, 139.0, 138.2, 128.1, 69.1, 66.7, 65.9 ppm. UV/Vis ($CHCl_3$): λ_{max} (ε/dm^3 mol^{-1} cm^{-1}) = 426 (6070), 326 (35520), 258 (122900) nm. MS (ESI): *m*/*z* = 1130.3 [M + H]$^+$, 1152.4 [M + Na]$^+$, 1168.3 [M + K]$^+$.

Compound 10: Ethylmalonyl chloride (409 mg, 2.7 mmol), dissolved in toluene (10 mL), was slowly added at 25 °C to a mixture of hydroxymethyl-18-crown-6 (800 mg, 2.7 mmol) and excess solid $NaHCO_3$ in toluene (50 mL). The mixture was stirred overnight under nitrogen and filtered without washing, and the solvent was removed at reduced pressure. The residue was purified by column chromatography (SiO_2; EtOAc/*i*PrOH, 2−15%, then EtOAc/MeOH, 2%) to give **10** as a colourless oil (590 mg, 53%). IR: $\tilde{\nu}$ = 2866, 1735, 1451, 1271, 1129 cm $^{-1}$. ^{1}H NMR ($CDCl_3$): δ = 4.18 (dd, 1 H, −COOCH_2CH−O−), 4.10 (m, 3 H, −COOCH_2CH−O− and −COOCH_2CH$_3$), 3.8−3.5 (m, 23 H, −OCH_2CH$_2$O−), 3.30 (s, 2 H, −OOCCH_2COO−), 1.2 (t, 3 H, −COOCH$_2$CH_3) ppm. ^{13}C NMR ($CDCl_3$): δ = 168.8, 166.2, 76.3, 70.6, 70.5, 70.3, 69.6, 64.6, 61.2, 41.2, 17.7, 13.8 ppm. $C_{18}H_{32}O_{10}$: calcd. C 52.9, H 7.9; found C 53.3, H 8.1.

Acknowledgments

The groups at the University of Bologna and Padova acknowledge partial support from the CNR in the programs "Materiali Innovativi (legge 95/95)" and Agenzia 2000 (CNRC00C4BD), the MIUR (MM03105353) and the University of Bologna ("Funds for Selected Research Topics"). The group in Pavia acknowledge the University of Pavia for financial support (FAR, 2000−2001), and Professors L. Fabbrizzi and A. Poggi for useful discussions and for the use of their apparatus for the transport experiments.

[1] [1a] M. Prato, *J. Mater. Chem.* **1997**, 1097−1109. [1b] (Ed.: A. Hirsch) *Fullerenes and Related Structures*, in *Top. Curr. Chem.* Springer-Verlag, Berlin/Heidelberg **1999**. [1c] K. M. Kadish, R. S. Ruoff, *Fullerenes: Chemistry, Physics, and Technology* J. Wiley, New York, **2000**. [1d]F. Wudl, *J. Mater. Chem.* **2002**, *12*, 1959−1963. [1e] *J. Mater. Chem.* **2002**, *12(7):* Special issue on functionalised fullerene materials. Guest Editors: M. Prato, N. Martín.

[2] [2a] H. Imahori, Y. Sakata, *Adv. Mater.* **1997**, *9*, 537−546. [2b] N. Martín, L. Sánchez, B. Illescas, I. Pérez, *Chem. Rev.* **1998**, *98*, 2527−2547. [2c] D. M. Guldi, *Chem. Soc. Rev.* **2002**, *31*, 22−36.

[3] [3a] P. A. van Hal, J. Knol, B. M. W. Langeveld-Voss, S. C. J. Meskers, J. C. Hummelen, R. A. J. Janssen, *Synth. Met.* **2001**, *166*, 123−127. [3b] D. Kuciauskas, P. A. Liddell, S. Lin, S. G. Stone, A. L. Moore, *J. Phys. Chem. B* **2000**, *104*, 4307−4321. [3c] D. M. Guldi, C. Luo, A. Swartz, M. Scheloske, A. Hirsch, *Chem. Commun.* **2001**, 1066−1067. [3d] J. L. Segura, N. Martín, *Tetrahedron Lett.* **1999**, *40*, 3239−3242.

[4] For examples of fullerene photovoltaics, see: [4a] N. S. Sariciftci, L. Smilowitz, A. J. Heeger, F. Wudl, *Science* **1992**, *258*, 1474−1476. [4b] G. Yu, J. Gao, J. C. Hummelen, F. Wudl, A. J. Heeger, *Science* **1995**, *270*, 1789−1791. [4c] J.-F. Eckert, J.-F. Nicoud, J.-F. Nierengarten, S.-G. Liu, L. Echegoyen, F. Barigelletti, N. Armaroli, L. Ouali, V. Krasnikov, G. Hadziioannou, *J. Am. Chem. Soc.* **2000**, *122*, 7467. [4d] C. J. Brabec, S. E. Shaheen, C. Winder, N. S. Sariciftci, P. Denk, *Appl. Phys. Lett.* **2002**, *80*, 1288.

[5] [5a] T. Da Ros, M. Prato, D. Guldi, E. Alessio, M. Ruzzi, L. Pasimeni, *Chem. Commun.* **1999**, 635−636. [5b] M. Gomez-Lopez, F. Diederich, *Chem. Soc. Rev.* **1999**, *28*, 263−277. [5c] E. Sartori, L. Garlaschelli, A. Toffoletti, C. Corvaja, M. Maggini, G. Scorrano, *Chem. Commun.* **2001**, 311−312. [5d] E. Sartori, A. Toffoletti, C. Corvaja, L. Garlaschelli, *J. Phys. Chem. A* **2001**, *105*, 10776−10780. [5e] V. Georgakilas, F. Pellarini, M. Prato, D. M. Guldi, M. Melle-Franco, F. Zerbetto, *Proc. Nat. Acad. Sci.* **2002**, *99*, 5075−5080. [5f] D. M. Guldi, N. Martín, *J. Mater. Chem.* **2002**, *12*, 1978−1992.

[6] [6a] J. S. Bradshaw, L. D. Hansen, S. F. Nielsen, M. D. Thompson, R. A. Reeder, R. M. Izatt, J. J. Christensen, *Chem. Commun.* **1975**, 874−75. [6b] J. S. Bradshaw, S. T. Jolley, B. A. Jones, *J. Heterocyclic. Chem.* **1980**, *17*, 1317−8. [6c] J. S. Bradshaw, G. E. Maas, J. D. Lamb, R. M. Izatt, J. J. Christensen, *J. Am. Chem. Soc.* **1980**, *102*, 467−474. [6d] R. M. Izatt, J. S. Bradshaw, S. A. Nielsen, J. D. Lamb, J. J. Christensen, *Chem. Rev.* **1985**, *85*, 271−339.

[7] G. Desimoni, G. Faita, M. Ricci, P. P. Righetti, *Tetrahedron* **1998**, *54*, 9581−9602.

[8] [8a] D. Pasini, P. P. Righetti, V. Rossi, *Org. Lett.* **2002**, *4*, 23−26. [8b] L. Garlaschelli, I. Messina, D. Pasini, P. P. Righetti, *Eur. J. Org. Chem.* **2002**, 3385−3392.

[9] [9a] F. Diederich, L. Isaacs, D. Philp, *Chem. Soc. Rev.* **1994**, *23*, 243−255. [9b] A. Hirsch, *Synthesis* **1995**, 895−913.

[10] [10a] S. R. Wilson, Y. Wu, *Chem. Commun.* **1993**, 784−86. [10b] U. Jonas, F. Cardullo, P. Belik, F. Diederich, A. Gügel, E. Hart, A. Herrmann, L. Isaacs, K. Müllen, H. Ringsdorf, C. Thilgen, P. Uhlmann, A. Vasella, C. A. A. Waldraff, M. Walter, *Chem. Eur. J.* **1995**, *1*, 243−251. [10c] Z. Guo, Y. Li, J. Yan, F. Bai, F. Li, D. Zhu, J. Si, P. Ye, *Appl. Phys. B, Lasers and Optics* **2000**, 257−60.

[11] Lewis acid-like cations such as Mg^{2+} are commonly used in combination with 1,3-dicarbonyl systems in asymmetric synthesis and catalysis.

[12] [12a] R. M. Izatt, J. S. Bradshaw, S. A. Nielsen, J. D. Lamb, J. J. Christensen, D. Sen, *Chem. Rev.* **1985**, *85*, 271−339. [12b] R. M. Izatt, K. Pawlak, J. S. Bradshaw, R. L. Bruening, *Chem. Rev.* **1991**, 1721−2085. [12c] G. Gokel, *Crown Ethers and Cryptands*, The Royal Society of Chemistry, Cambridge, **1991**.

[13] G. D. Beresford, J. F. Stoddart, *Tetrahedron Lett.* **1980**, *21*, 867−870.

[14] [14a] K. E. Koenig, G. M. Lein, P. Stuckler, T. Kaneda, D. J. Cram, *J. Am. Chem. Soc.* **1979**, *101*, 3553−3566. [14b] K. A. Connors, *Binding Constants* John Wiley & Sons: New York, **1987**.

[15] [15a] J. S. Bradshaw, R. M. Izatt, *Acc. Chem. Res.* **1997**, *30*, 338−345. [15b] G. De Santis, M. Di Casa, L. Fabbrizzi, A. Forlini, M. Licchelli, C. Mangano, J. Mocàk, P. Pallavicini, A.

Poggi, B. Seghi, *J. Coord. Chem.* **1992**, *27*, 39−73. [15c] G. De Santis, M. Di Casa, M. Mariani, B. Seghi, L. Fabbrizzi, *J. Am. Chem. Soc.* **1989**, *111*, 2422−2427. [15d] Y. Habata, K. Uchida, Y. Sato, S. Akabori, *J. Membr. Sci.* **1993**, *85*, 175−181. [15e] A. J. Wright, S. E. Matthews, W. B. Fisher, P. D. Beer, *Chem. Eur. J.* **2001**, *7*, 3474−3481. [15f] L. A. Barnhurst, A. G. Kutateladze, *Org. Lett.* **2001**, *3*, 2633−2635.

[16] The initial transport rate is linear, but the behaviour becomes nonlinear as the back transport rate becomes competitive. Eventually, when both the source and receiving aqueous phases contain the same amount of picrate salt, rate of transport and back transport should equilibrate. See ref. 15b for a clear, exhaustive discussion.

[17] On stirring a solution of fullerene derivative **7b** in $CHCl_3$ (10^{-3} M) in the presence of two layers of distilled H_2O in the transport cell, no partition in the upper layers could be detected by UV/Vis spectroscopy.

[18] C. Corvaja, M. Maggini, M. Prato, G. Scorrano, M. Venzin, *J. Am. Chem. Soc.* **1995**, *117*, 8857−8858.

[19] TR-EPR spectra were also recorded with 4-ammonium-2,2,6,6-tetramethyl-1-piperidinyloxy free radical (ammonium-TEMPO) with similar results. With this radical, however, less resolved quadruplet spectral features were obtained, possibly because the larger steric hindrance influences the kinetics of the complexation equilibrium.

[20] S. K. Wong, D. A. Hutchinson, J. K. S. Wan, *J. Phys. Chem.* **1973**, *58*, 985−989.

[21] [21a] K. Obi, T. Imamura, *Rev. Chem. Intermed.* **1986**, *7*, 225−242. [21b] T. Imamura, O. Onitsuka, K. Obi, *J. Phys. Chem.* **1986**, *90*, 6741−6744. [21c] J. Fujisawa, K. Ishii, Y. Ohba, M. Iwaizumi, S. Yamauchi, *J. Phys. Chem.* **1995**, *99*, 17082−17084. [21d] J. Fujisawa, K. Ishii, Y. Ohba, S. Yamauchi, M. Fuhs, K. Möbius, *J. Phys. Chem. A* **1997**, *101*, 5869−5876. [21e] I. S. M. Saiful, J. Fujisawa, N. Kobayashi, Y. Ohba, S. Yamauchi, *Bull. Chem. Soc. Jpn.* **1999**, *72*, 661−667. [21f] A. Blank, H. Levanon, *J. Phys. Chem.* **2000**, *104*, 794−800.

[22] [22a] C. Blättler, F. Jent, H. Paul, *Chem. Phys. Lett.* **1990**, *166*, 375. [22b] A. Kawai, T. Okutsu, K. Obi, *J. Phys. Chem.* **1991**, *95*, 9130−9134. [22c] A. Kawai, K. Obi, *J. Phys. Chem.* **1992**, *96*, 52. [22d] A. Kawai, K. Obi, *J. Phys. Chem.* **1992**, *96*, 5701−5704. [22e] A. I. Shushin, *Zeit. Physik. Chem.* **1993**, *182*, 9−18. [22f] G.-H. Goudsmit, H. Paul, A. I. Shushin, *J. Phys. Chem.* **1993**, *97*, 13243−13249.

[23] [23a] K. M. Salikhov, Y. N. Molin, R. Z. Sagdeev, A. L. Buchachenko, in *Spin Polarisation and Magnetic Effects in Radical Reactions*, (Ed.: Molin, Y., Elsevier, Amsterdam, **1984**, p. 324.[23b]M. Mazzoni, F. Conti, C. Corvaja, *Appl. Magn. Reson.* **2000**, *18*, 351−361.

[24] A. Bencini, D. Gatteschi, *EPR of exchange coupled systems*, Springer Verlag, Berlin, **1990**, pp. 53−55.

[25] [25a] F. Paolucci, M. Marcaccio, S. Roffia, G. Orlandi, F. Zerbetto, M. Prato, M. Maggini, G. Scorrano, *J. Am. Chem. Soc.* **1995**, *117*, 6572−6580. [25b] M. Carano, P. Ceroni, L. Mottier, F. Paolucci, S. Roffia, *J. Electrochem. Soc.* **1999**, *146*, 3357−3360. [25c] S. Cattarin, P. Ceroni, D. M. Guldi, M. Maggini, E. Menna, F. Paolucci, S. Roffia, G. Scorrano, *J. Mater. Chem.* **1999**, *9*, 2743−2750.

[26] [26a] M. W. J. Beulen, J. A. Rivera, M. Á. Herranz, Á. Martín-Domenech, N. Martín, L. Echegoyen, *Chem. Commun.* **2001**, 407−8. [26b] M. W. J. Beulen, L. Echegoyen, J. A. Rivera, M. Á. Herranz, Á. Martín -Domenech, N. Martín, *Chem. Commun.* **2000**, 917−8. [26c] R. Kessinger, J. Crassous, A. Herrmann, M. Rüttiman, L. Echegoyen, F. Diederich, *Angew. Chem. Int. Ed.* **1998**, *37*, 1919−1922. [26d] Á. Herranz, M. W. J. Beulen, J. A. Rivera, L. Echegoyen, M. C. Díaz, B. M. Illescas, N. Martín, *J. Mater. Chem.* **2002**, *12*, 2048−2053.

[27] [27a] B. Knight, N. Martín, T. Ohno, E. Ortí, C. Rovira, J. Veciana, J. Vidal-Gancedo, P. Viruela, R. Viruela, F. Wudl, *J. Am. Chem. Soc.* **1997**, *109*, 9871−9882. [27b] ref. 2b.

[28] M. Carano, L. Echegoyen, manuscript in preparation.

[29] [29a] B. Knight, N. Martín, T. Ohno, E. Ortí, C. Rovira, J. Veciana, J. Vidal-Gancedo, P. Viruela, R. Viruela, F. Wudl, *J. Am. Chem. Soc.* **1997**, *109*, 9871−9882. [29b] ref.[2b].

[30] N. Camaioni, L. Garlaschelli, A. Geri, M. Maggini, G. Possamai, G. Ridolfi, *J. Mat. Chem.* **2002**, *12*, 2065−2070.

[31] J. Mitchell, W. M. D. Bryant, *J. Am. Chem. Soc.* **1943**, *65*, 128−137.

Received July 11, 2002
[O02387]